DRAFT
Submitted to JCP 10/08/02
UCRL JC-148873

Solution of the nonlinear multigroup radiation diffusion equation using multigrid and pseudo transient continuation*

Aleksei I. Shestakov
Lawrence Livermore National Laboratory
Livermore CA 94550

March 17, 2003

Address correspondence to:
Aleksei I. Shestakov
Lawrence Livermore National Laboratory
P.O. Box 808, L-38
Livermore, CA 94551
(925) 422-4213
(925) 423-9208 (FAX)
shestakov@llnl.gov

*This work was performed under the auspices of the U.S. Department of Energy by the University of California Lawrence Livermore National Laboratory under contract No. W-7405-Eng-48.

Abstract

We present a numerical solution for the system coupling the multigroup radiation diffusion and the matter energy balance equations. The scheme is applied to a nondimensional model which specifies an ideal gas equation of state. Opacities are proportional to the inverse of the cube of the frequency, thereby simulating free-free transitions. Radiation emission is given by a Wien spectrum. The method consists of a multigrid approach whereby the solution on coarse levels of groups is interpolated to finer levels. On each level, we obtain a nonlinear system of equations which incorporates the groups' diffusive transport and their inter group coupling. After linearizing, to ensure robustness, we introduce pseudo transient continuation and obtain an M matrix and a nonnegative right side. The linear system is solved by an iterative technique based on two regular splittings of the matrix. The iteration symbol is analyzed and shown to be convergent for a wide range of time steps. The scheme is applied to two problems. One simulates the diffusive transport and equilibration of a localized energy source. The second models the propagation of energy through initially cold material.

Keywords. nonlinear PDE of parabolic type, numerical linear algebra, boundary value problems, finite difference methods, multigrid methods, astronomy and astrophysics, radiative transfer

AMS subject classification. 35K55, 35Q99, 65F10, 65H10, 65H20, 65N06, 65N12, 65N55, 85-08, 85A25

1 Introduction

In this paper we develop a numerical scheme for the nondimensional multifrequency radiation diffusion equations derived by Hald & Shestakov (H&S) [1],

$$\partial_t u = \nabla \cdot \nu^3 \nabla u + (B_\nu - u) / \nu^3 , \tag{1}$$

$$R \, \partial_t T = -T + \int_0^\infty (u/\nu^3) \, d\nu , \tag{2}$$

In (1)–(2), $u = u(x, t, \nu)$ and $T = T(x, t)$ represent the spectral radiation energy density and matter temperature respectively. In the H&S model, matter emits radiation according to a Wien spectrum. Thus,

$$B_\nu = \nu^3 e^{-\nu/T} . \tag{3}$$

The independent variables x, t, and ν denote distance, time, and frequency respectively; R is a positive constant.

For numerical computations, the frequency spectrum is discretized into $\mathcal{N}$ *groups*,

$$0 = \nu_0 < \nu_1 < \nu_2 < \cdots < \nu_{\mathcal{N}} ,$$

where $\nu_{\mathcal{N}}$ is assumed to be "large enough." To be precise, $\nu_{\mathcal{N}}$ should be so large that at all times, the radiation at higher frequencies is negligible, i.e.,

$$\int_0^\infty u_\nu \, d\nu = \int_0^{\nu_{\mathcal{N}}} u_\nu \, d\nu .$$

Let

$$\Delta_j \doteq \nu_j - \nu_{j-1} .$$

define the group widths. We assume that the widths are sufficiently fine and cover a wide range so that at all times

$$\nu_1 / T \ll 1 \ll \nu_{\mathcal{N}} / T .$$

By integrating (1) over each group, we obtain $\mathcal{N}$ equations, one per group. Defining the jth integral operator,

$$\int_j \doteq \int_{\nu_{j-1}}^{\nu_j} d\nu ,$$

we derive each term. Thus,

$$\int_j \partial_t u = \partial_t \int_j u \doteq \partial_t u_j$$

where u_j represents the integral of the spectral radiation density over the jth group.[1] For the transport term,

$$\int_j \nabla \nu^3 \nabla u_\nu = \nabla \cdot \hat{\nu}_j^3 \nabla u_j ,$$

[1] The definition implies that u and u_j have different "dimensions;" the former is in units of energy density per frequency; the latter is an energy density.

while for the absorption term,

$$\int_j u_\nu/\nu^3 = (\bar{\nu}_j)^{-3}\, u_j \ ,$$

where $\hat{\nu}_j$ and $\bar{\nu}_j$ satisfy,

$$\nu_{j-1} < \hat{\nu}_j \ , \ \bar{\nu}_j < \nu_j \ . \tag{4}$$

Equation (3) leads to

$$\int_j B_\nu/\nu^3 = \int_j (\nu^3 e^{\nu/T})/\nu^3 = p_j\, T \ ,$$

where

$$p_j \doteq \exp(-\nu_{j-1}/T) - \exp(-\nu_j/T) \ . \tag{5}$$

By defining

$$\bar{\mu}_j \doteq (\bar{\nu}_j)^3 \ , \ \ \hat{\mu}_j \doteq (\hat{\nu}_j)^3 \ ,$$

and discretizing the integral in (2), we obtain the multigroup system of $\mathcal{N}+1$ equations,

$$\partial_t u_j \ = \ \nabla \cdot \hat{\mu}_j \nabla u_j + p_j\, T - u_j/\bar{\mu}_j \ , \ \ (\, j = 1, \ldots, \mathcal{N}\,) \, , \tag{6}$$

$$R\, \partial_t T \ = \ -T + \sum_{j=1}^{\mathcal{N}} u_j/\bar{\mu}_j \ . \tag{7}$$

The one–group system is obtained by integrating once over all frequencies. To this end, we note that for (1)–(2), the so-called equilibrium or stationary solution arises as $u \to B_\nu$. If we integrate (1)–(2) and follow the usual analogues of "Planck" averaging the coupling coefficient ν^{-3} [2], p.166, and "Rosseland" averaging the diffusion coefficient ν^3 [2], p.153, *but averaging with the equilibrium function* $\nu^3\, e^{-\nu/T}$, we obtain,

$$\partial_t E \ = \ \nabla \cdot 210\, T^3\, \nabla E + (\, 6T^4 - E\,) \,/\, (6T^3) \, , \tag{8}$$

$$R\, \partial_t T \ = \ -\,(\, 6T^4 - E\,) \,/\, (6T^3) \, , \tag{9}$$

where $E = \int d\nu\, u$ represents the radiation energy density.

The three systems (1)–(2), (6)–(7), and (8)–(9) preserve important properties of the commonly used (dimensional) radiation diffusion equations. Ignoring boundary fluxes (accomplished by imposing homogeneous Neumann boundary conditions on u or E), the total energy is constant. For the systems (1)–(2), (6)–(7), and (8)–(9), the total energy density is $RT + \int d\nu\, u$, $RT + \sum_j u_j$, and $RT + E$ respectively. The high frequency photons, i.e., u with large ν in (1)–(2) or u_j/Δ_j with large j in (6)–(7), are characterized by fast transport and slow absorption. In (1), $1/\nu^3$ plays the role of a coupling coefficient, with low frequencies coupling the fastest. Matter preferentially emits radiation into frequencies where $\nu^3\, e^{-\nu/T}$ is maximal. Analogously, (6) shows that radiation absorption is proportional to $\bar{\mu}_j^{-1}$ while radiation emission[2] is greatest into the group with maximum $p_j T/\Delta_j$.

[2] measured in "units" of energy/volume/frequency

We now resolve the discrepancy between the variables $\hat{\mu}_j$ and $\bar{\mu}_j$ in (6)–(7). For the absorption, the analogue of Planck averaging over a group yields

$$\begin{aligned}\int_j u/\nu^3 &= \left(\int_j u\right)\left(\int_j B_\nu(T)\,/\,\nu^3\right)\Big/\left(\int_j B_\nu(T)\right)\\ &\doteq u_j\,(\bar{\nu}_j)^{-3}\,.\end{aligned}$$

After integrating, we obtain,

$$1/\bar{\mu}_j = (\bar{\nu}_j)^{-3} = \frac{1}{T^3}\,\frac{e^{-y}\,|_{y=y_{j-1}}^{y_j}}{e^{-y}\,q_3(y)|_{y=y_{j-1}}^{y_j}}\ ,\ \ y_j = \nu_j/T\ , \tag{10}$$

where, for $m \geq 0$,

$$q_m(y) = m!\sum_{\ell=0}^{m} y^\ell/\ell!\,.$$

For the transport, the analogue of Rosseland averaging gives,

$$\begin{aligned}\int_j \nu^3\nabla u &= \left(\int_j \nabla u\right)\left(\int_j \nu^3\nabla B_\nu\right)\Big/\left(\int_j \nabla B_\nu\right)\\ &= \nabla u_j\,\left(\int_j \nu^3\,\partial B_\nu/\partial T\right)\Big/\left(\int_j \partial B_\nu/\partial T\right)\\ &\doteq (\hat{\nu}_j)^3\,\nabla u_j\,.\end{aligned}$$

After integrating, we obtain

$$\hat{\mu}_j = (\hat{\nu}_j)^3 = T^3\,\frac{e^{-y}\,q_7(y)|_{y=y_{j-1}}^{y_j}}{e^{-y}\,q_4(y)|_{y=y_{j-1}}^{y_j}}\ ,\ \ y_j = \nu_j/T\,. \tag{11}$$

Equations (10) and (11) imply that $\hat{\nu}_j$ and $\bar{\nu}_j$ depend on T which may equal any non-negative value. The dependence appears to contradict the requirement (4) since the frequency mesh $\{\nu_j\}$ is fixed. In Appendix A we show that (4) is always satisfied and that the dependence on T is somewhat benign, especially for large $\mathcal{N}$. To illustrate, in the limit of small frequency mesh width,

$$\lim_{\Delta_j\to 0}\bar{\mu}_j = \nu_{j-1}^3 + (3/2)\,\nu_{j-1}^2\,\Delta_j + \left(\frac{4-\nu_{j-1}/T}{4}\right)\,\nu_{j-1}\,(\Delta_j)^2 + \dots\ ,\ .$$

The coefficient $\hat{\mu}_j$ has a similar expansion and the difference,

$$\lim_{\Delta_j\to 0}(\,\hat{\mu}_j - \bar{\mu}_j\,) = \nu_{j-1}\,(\Delta_j)^2 + (\Delta_j)^3/2 + \dots\ .$$

However, when Δ_j is large, the diffusion and coupling coefficients $\hat{\mu}_j$ and $\bar{\mu}_j$ of (6)–(7) have a larger temperature dependence. For small $\mathcal{N}$, the difference $\hat{\mu}_j - \bar{\mu}_j$ is more pronounced. The effect is dramatically illustrated by (8)–(9) (for which $\mathcal{N} = 1$) in which the roles of $\hat{\mu}_j$ and $\bar{\mu}_j$ are played by $210T^3$ and $6T^3$ respectively.

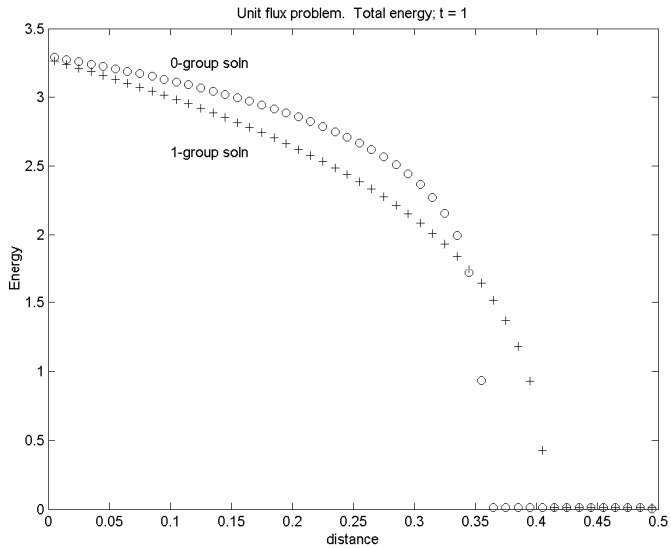

Figure 1: Unit flux problem. 0-group energy density RT and 1-group energy density $RT + E$ vs. x; $R = 10$.

Solutions of (8)–(9) and (6)–(7) are markedly different. Consider the semi infinite interval: $0 < x < \infty$. Assume that initially, $u = E = T = 0$ and that at $x = 0$ we impose a constant, unit flux of energy into the radiation field. After some time, for (8)–(9), a steep front develops. At the edge of the front, where T is still cold, $E \approx 6T^4$ (due to the large coupling coefficient). If (8) and (9) summed, assuming $E \ll RT$ and substituting $E = 6T^4$, we obtain,

$$R\,\partial_t T = \partial_x \left(5040\,T^6\,\partial_x T\right) , \tag{12}$$

i.e., the front propagates as a thermal wave [2]. Solutions of (8)–(9) and (12) are remarkably similar; they are displayed in Fig. 1. The "0-group" refers to the solution of (12). The 1-group energy refers to $RT + E$ of (8)–(9).

On the other hand, solutions of (6)–(7) will not have a sharp front. Some energy is deposited into the high frequency groups, either by the boundary condition, or by the matter. These groups are characterized by large diffusion and small absorption coefficients. Hence, this energy propagates deep into the domain before it is absorbed.

In the following sections we first present a general description of the method. The fundamental concept is to apply multigrid to the frequency coordinate. We construct a hierarchy of ν grids. On each *level*, we advance N $(\leq \mathcal{N})$ diffusion equations which are coupled through the matter temperature T. After these equations are time–advanced, the result is interpolated to the next finer level using the procedure described in section 3. Section 4 describes how the level equations are linearized. We introduce pseudo transient continuation Ψtc in order to obtain a robust linear system $Ax = b$

for the radiation energy densities. Section 5 proves that a judicious choice of the Ψtc parameter ensures that A is an M–matrix and b is nonnegative. The system is solved by iterations. A dual matrix splitting alternates between solving systems of size equal to the number of spatial grid points, and systems of size equal to the number of groups in a level. Section 6 proves that the iteration matrices are convergent. Results appear in section 7. Two problems are considered; one simulates the diffusion of a localized source of matter energy while the other, the propagation of radiation into cold matter. Concluding remarks appear in section 8.

Before launching into the overview, we review the three methods commonly used to solve the multigroup equations. All are of semi–implicit form; coefficients such as the specific heat and opacities are evaluated at the old time level. Furthermore, the schemes are at best linear; the emission term is linearized about the old temperature. The simplest method is the "partial temperature" (PT) scheme of Lund and Wilson [3], [4]. The PT scheme is an application of operator splitting. For each time step, each group is addressed only once. Thus, the PT scheme cannot even be said to solve a linearization of the equations. The other two methods do indeed attempt to solve linear systems coupling all of the radiation groups to a linearization of the emission term. One method, dubbed "fully implicit" (FI) is the scheme of Axelrod et al [5]. Friedman and Kershaw [6] extended the FI scheme for spatially 2D computer programs. Lastly, is the scheme of Morel et al [7] which begins with the same linearization as the FI scheme, but algebraically eliminates the matter temperature thereby obtaining a system that explicitly couples all of the groups. The system is solved by an acceleration technique that ignores the diffusive transport. Readers familiar with the FI and Morel schemes will note distinct similarities with ours. Indeed, the method proposed in this paper attempts to incorporate the best features of each.

2 Overview of scheme

Given initial conditions at $t = t^n$, our job is to produce a solution for the (nonlinear) system (6)–(7) at $t^{n+1} = t^n + \Delta t$ where the time step Δt may be arbitrarily large. In order to avail ourselves of fast, robust methods, we limit the complexity of the underlying linear system solver to one that tackles nothing more complicated than a discretization of a single, scalar elliptic equation of the form,

$$\nabla \cdot a \nabla u - b\, u = w \ .$$

For sufficiently large 2D and 3D meshes, especially if running on massively parallel platforms, such systems are typically solved by iterating. And, since iterations only refine initial guesses, it is useful to have a good initial iterate, i.e., a good guess for the fields at $t = t^{n+1}$. If Δt is sufficiently large, the value at $t = t^n$ may be inadequate.

Although our method may be applied to discretizations using an arbitrary number of groups $\mathcal{N}$, for simplicity, we assume that $\mathcal{N}$ is a power of two.

The scheme's premise is that if we had already time–advanced the solution using $\mathcal{N}/2$ groups, then this coarse level solution should be a good guess for the problem

using $\mathcal{N}$ groups *if* the coarse level is properly interpolated to the fine level. The idea is recursive. The solution using $\mathcal{N}/2$ groups, which may still be expensive to obtain, may itself be approximated by time advancing a system of $\mathcal{N}/4$ groups. Taking this to the limit, one arrives at the "coarsest" *level* of groups, which in this paper we assume to be the "one group" system (8)–(9). Although robust methods for the one-group equations are readily available, e.g., [8], for completeness, we present one in Appendix B.

Thus, given a frequency grid of $\mathcal{N}$ groups, we construct a hierarchy of coarse levels, e.g., of $\mathcal{N}/2$, $\mathcal{N}/4$, etc., groups spanning the same frequency range. We assume that the coarse and fine levels use the same spatial grid.[3] Since we bootstrap to finer (frequency) levels, the temperature T obtained on the coarse level forms the initial guess on the fine level. For the radiation field, we interpolate the coarse level as described in section 3. To summarize, each time-advancement consists of the following steps.

1. Advance coarsest level equations to desired accuracy. Ensure that time advanced solution conserves energy.
2. Interpolate result to finer level to form initial guess.
3. On each level, perform outer iterations.
   - Compute coefficients, e.g., opacities.
   - Linearize equations.
   - Compute Ψtc parameter τ to ensure robustness of linear system.
   - Solve linear system (using iterations) to desired accuracy.
4. Check (nonlinear) convergence. If desired accuracy is reached, exit level with energy conserving fields.

Steps 2–4 are repeated until we reach the finest level.

This concludes the overview. In the following sections we describe the procedures in greater detail.

3 Coarse–fine interpolation

We now discuss how we interpolate a coarse level solution to the fine level. Since we only refine the frequency coordinate, the time advanced temperature on the coarse level forms the initial guess on the fine level. For the radiation field, we interpolate as follows. Let $\{\nu_{j-1}, \nu_j, \nu_{j+1}\}$ denote a refinement of a single coarse frequency mesh width $\{\nu_{j-1}, \nu_{j+1}\}$ and let $u^c_{j_c}$ represent the solution over the coarse interval.

[3] The coarse level may use a coarsened spatial grid. In this case, we resort to classical multigrid and interpolate the coarse (spatial) grid solution to the fine grid.

We assume a local equilibrium exists over the interval and solve for the "radiation" temperature Θ_{j_c} which satisfies

$$\begin{aligned} u^c_{j_c} &= \int_{\nu_{j-1}}^{\nu_{j+1}} d\nu\, \nu^3\, e^{-\nu/\Theta_{j_c}} \\ &= (\Theta_{j_c})^4\, [\, e^{-y_{j-1}} q_3(y_{j-1}) - e^{-y_{j+1}} q_3(y_{j+1})\,] \,, \end{aligned} \tag{13}$$

where $y_{j\pm1} = \nu_{j\pm1}/\Theta_{j_c}$. The variable Θ_{j_c} is obtained using Newton's method. We initialize the Newton iterations with $\Theta_{j_c} = \Theta_{j_c-1}$, i.e., with the Θ value obtained from the previous coarse width. If $j = 1$, we initialize with $\Theta_{j_c} = T$, the coarse level matter temperature. Clearly, if the problem is near equilibrium, the Newton iterations converge quickly and, furthermore, the fine level is initialized with an excellent guess.

After the Newton iterations have converged, the initial guesses $u^{(0)}_j$, $u^{(0)}_{j+1}$ are found by integrating the assumed local equilibrium, i.e.,

$$u^{(0)}_i = \int_{\nu_{i-1}}^{\nu_i} d\nu\, \nu^3\, e^{-\nu/\Theta_{j_c}} \quad , \quad (\, i = j,\, j+1\,) \,.$$

We caution that the above procedure is not robust. If $u^c_{j_c}$ is sufficiently large, there is no solution.[4] In case of such failure, we revert to "constant interpolation." That is, we assume that the spectral energy density, as approximated by the coarse solution $u^c_{j_c}$, is constant over the coarse interval. Then, by defining the grid fraction

$$f = (\nu_j - \nu_{j-1})/(\nu_{j+1} - \nu_{j-1}) \,,$$

we set,

$$u^{(0)}_j = f\, u^c_{j_c} \;\text{ and }\; u^{(0)}_{j+1} = (1-f)\, u^c_{j_c} \,.$$

4 Derivation of linear system

Here we derive the linear system for the multigroup frequency levels. Let N denote the number of groups of the current level. After discretizing the temporal derivatives of (6)–(7) and multiplying by Δt, we obtain

$$0 = -(\, u_j - u^0_j\,) + \Delta t\, (\, \nabla \cdot \hat{\mu}_j \nabla u_j + p_j\, T - u_j/\bar{\mu}_j\,) \,, \tag{14}$$

$$0 = -R\,(\, T - T^0\,) + \Delta t \left(-T + \sum_{j=1}^{N} u_j/\bar{\mu}_j \right) \,, \tag{15}$$

where $j = 1, \ldots, N$. Equations (5), (10), and (11) show that p_j, $\bar{\mu}_j$, and $\hat{\mu}_j$ depend on T.

[4] The nonrobustness is due to our choosing to give B a Wien distribution. For the Planck function, $B = B_P = \nu^3/(\exp(-\nu/\Theta) - 1)$. For large Θ, $B_P \approx \nu^2\, \Theta\, (1 - \nu/2\Theta)$, i.e., for any ν, B_P can be arbitrarily large. Thus, if $B = B_P$, the analogue of (13) can be solved for arbitrarily large $u^c_{j_c}$. However, for the Wien distribution B_W, if Θ is large, $B_W \approx \nu^3\, (1 - \nu/\Theta)$, which puts a bound on B_W [9].

Treating Δt as a parameter, we view (14)–(15) as a *time independent* system and replace the zeroes on the left hand side (LS) with pseudo–time derivatives $\partial u_j/\partial\tau$ and $R\,\partial T/\partial\tau$. Thus, the solution of (14)–(15) is the steady state of the pseudo–time dependent equations. The need for the pseudo–time derivatives, in particular the utility of τ, the inverse of the pseudo–time step,

$$0 \le \tau \doteq 1/\Delta\tau < \infty \ ,$$

will be made evident in Section 5. For the moment, we note that setting $\tau = 0$ returns (14)–(15). However, a positive τ yields the following discretization of the temperature equation,

$$R\,\tau\,(\,T - T^{(i)}\,) \ = -R\,(\,T - T^0\,) + \Delta t\,\left(\,-T + \sum_{j=1}^{N} v_j\,\right) \ ,$$

where $T^{(i)}$ is the temperature at the previous pseudo–time and where we have introduced

$$v_j \doteq u_j/\bar{\mu}_j \ .$$

Henceforth, v_j, which is also nonnegative, will be the unknown of interest.

Solving for T yields

$$T = \gamma_\tau\,T^{(i)} + (1 - \gamma - \gamma_\tau)\,T^0 + \gamma \sum_{j=1}^{N} v_j \ , \tag{16}$$

where,

$$0 < \gamma = \ \frac{\Delta t}{R\,\tau + R + \Delta t} \ < 1 \ , \tag{17}$$

$$0 \le \gamma_\tau = \ \frac{R\,\tau}{R\,\tau + R + \Delta t} \ < 1 \ . \tag{18}$$

Equation (16) is robust. Once nonnegative v_j are computed, the temperature T is an average of the radiation energies, the old temperature T^0, and the intermediate $T^{(i)}$.

For the v_j equations, in order to avoid ill posed systems, we do not linearize the $\bar{\mu}_j$ and $\hat{\mu}_j$ coefficients, but instead evaluate them at the temperature $T^{(i)}$. However, we do expand the emission $p_j\,T$ in (14) about $T^{(i)}$. Thus,

$$p_j T = \alpha_j^{(i)}\,T + (p_j^{(i)} - \alpha_j^{(i)})\,T^{(i)} \ , \tag{19}$$

where

$$\alpha_j^{(i)} = (1 + y_{j-1}^{(i)})e^{-y_{j-1}^{(i)}} - (1 + y_j^{(i)})e^{-y_j^{(i)}} \ ,$$

and $y_j^{(i)} = \nu_j/T^{(i)}$. Note that for all j and $T^{(i)} \ge 0$,

$$0 < \alpha_j^{(i)} < 1 \quad \text{and} \quad \sum_{j=1}^{N} \alpha_j^{(i)} = 1 \ . \tag{20}$$

Similar expansions are readily derived for $p_j^{(i)}$. The main point is that, because of their dependendence on T, p and α depend on position x.

Equation (19) enables eliminating T from (14); the emission and absorption terms become,

$$\begin{aligned} p_j\, T - u_j/\bar{\mu}_j &= \gamma\, \alpha_j \sum_{\ell=1}^{N} v_\ell \\ &+ \alpha_j (1-\gamma-\gamma_\tau)\, T^0 + [\alpha_j(\gamma_\tau - 1) - p_j]\, T^{(i)} - v_j \ . \end{aligned} \tag{21}$$

where we have suppressed the superscripts of α_j and p_j. If we substitute (21) into (14), we obtain a set of equations involving only the unknowns v_j. On the LS of (21), we include the pseudo–temporal derivative

$$\tau\, \bar{\mu}_j\, (\, v_j - v_j^{(i)}\,) \ .$$

In the following, without loss of generality, we assume a one dimensional spatial domain and let $\{x_{k+1/2}\}$ define the grid points. Thus, $h_k \doteq x_{k+1/2} - x_{k-1/2}$ is the "volume "of the $k^{\rm th}$ cell and $x_{k\pm 1/2}$ are its "edges." The unknowns $v_{k,j}$ represent the radiation energy density of the $j^{\rm th}$ group in the $k^{\rm th}$ cell divided by the cube of an average frequency. In terms of $v_{k,j}$, the discretization of the flux term over the $k^{\rm th}$ cell is given by

$$\begin{aligned} \Delta t\, \nabla\cdot \hat{\mu}_j \nabla u_j &= \frac{\Delta t}{h_k} \left[\hat{\mu}_{k+1/2,j}\, \frac{u_{k+1,j} - u_{k,j}}{h_{k+1/2}} - \hat{\mu}_{k-1/2,j}\, \frac{u_{k,j} - u_{k-1,j}}{h_{k-1/2}} \right] \\ &= \frac{\Delta t}{h_k} \left[\frac{\hat{\mu}_{k+1/2,j}\, \bar{\mu}_{k,j}}{h_{k+1/2}} \left(\frac{\bar{\mu}_{k+1,j}}{\bar{\mu}_{k,j}}\, v_{k+1,j} - v_{k,j} \right) \right. \\ &\qquad \left. - \frac{\hat{\mu}_{k-1/2,j}\, \bar{\mu}_{k,j}}{h_{k-1/2}} \left(v_{k,j} - \frac{\bar{\mu}_{k-1,j}}{\bar{\mu}_{k,j}}\, v_{k-1,j} \right) \right] \ . \end{aligned}$$

Note that because of the dependence on T, the coefficients $\hat{\mu}_j$ and $\bar{\mu}_j$ have a spatial index k (with the proper centering.) However, (10), (11), and (4) imply that that the spatial variation is mild—especially for refined spectral grids. Hence, in order to analyze the linear iterative scheme, we drop the spatial indexing of $\hat{\mu}_j$ and $\bar{\mu}_j$.[5] If we assume a uniform spatial grid ($h = h_k = h_{k\pm 1/2}$) and define

$$\eta_j \doteq \Delta t\, \hat{\mu}_j\, \bar{\mu}_j / h^2 \ ,$$

then, the flux term reduces to the simple form

$$\Delta t\, \nabla\cdot \hat{\mu}_j \nabla u_j = \eta_j\, (\, v_{k+1,j} - 2v_{k,j} + v_{k-1,j}\,) \ .$$

Combining the above discretizations yields the linear system

$$-\eta_j\, (\, v_{k+1,j} - 2v_{k,j} + v_{k-1,j}\,) + d_j\, v_{k,j} - \gamma\, \Delta t\, \alpha_{k,j} \sum_{\ell=1}^{N} v_{k,\ell} = w_{k,j} \ , \tag{22}$$

[5] The computer program retains the spatial dependence $\hat{\mu}_{k-1/2,j}$ and $\bar{\mu}_{k,j}$.

where

$$d_j = (1+\tau)\bar{\mu}_j + \Delta t \quad \text{and} \tag{23}$$

$$\begin{aligned} w_{k,j} &= (\,\tau\, v_{k,j}^{(i)} + v_{k,j}^{0}\,)\,\bar{\mu}_j + \\ &\quad \Delta t\,\{\,\alpha_{k,j}(1-\gamma-\gamma_\tau)\,T_k^0 + [p_{k,j} + \alpha_{k,j}(\gamma_\tau - 1)]\,T_k^{(i)}\,\}\,. \end{aligned} \tag{24}$$

5 Analysis of linear system

Equation (22) is of the form $Av = w$ where v and w are the vectors with components $v_{k,j}$ and $w_{k,j}$, respectively. The diagonal of A is positive and all offdiagonal entries are nonnegative. If A were to be an M-matrix, i.e., if the elements of A^{-1} were nonnegative, and if all components of w were also nonnegative, the system $Av = w$ would be robust. That is, the new energies would be physically reasonable.

In this section we show that a judicious choice of τ guarantees robustness. Before plunging into the analysis, it is useful to note several points about (22). Our job is to produce physically reasonable v for any choice of parameters and RS. In particular, we assume that we are unable to change Δt, the physical time step.[6] Furthermore, even if we could change it, e.g., by lowering it in order to ensure diagonal dominance, we must anticipate the possibility that for $\tau = 0$, $w_{k,j}$ may be negative for sufficiently small v^0 and T^0 because of the indeterminacy of the sign of the coefficient multiplying $T_k^{(i)}$.

To guarantee the M-matrix property, we recall Varga [11], Theorem 3.11, Corollary 1, p. 85, which states that A is an M-matrix if it is irreducibly diagonally dominant and consists of positive diagonal and nonnegative offdiagonal entries. Irreducibility may be proved by showing that the directed graph of A is strongly connected, Varga [11], Theorem 1.6, p. 20, and the latter is easily done by inspection. Diagonal dominance is proved by the following lemma which derives a condition for τ. The lemma introduces a "safety factor" $\beta > 0$ which we discuss in the remarks.

Lemma 1 *Let $\beta \geq 0$. Define*

$$\begin{aligned} a &= R\,\bar{\mu}_j\,, \\ b &= 2\,R\,\bar{\mu}_j + \Delta t\,[\,\bar{\mu}_j + R\,(1-\beta)\,]\,, \quad \text{and} \\ c &= R\,\bar{\mu}_j + \Delta t\,[\,\bar{\mu}_j + R\,(1-\beta)\,] + \Delta t^2\,(\,1 - N\alpha_{k,j} - \beta\,)\,. \end{aligned}$$

If $\beta \leq 1$ and $c \geq 0$, then A is diagonally dominant for all $\tau \geq 0$. Otherwise, A is diagonally dominant if

$$\tau \geq (\,\sqrt{b^2 - 4ac} - b\,)/2a\,. \tag{25}$$

Remark Diagonal dominance is attained just with $\beta = 0$. A positive β adds a margin of safety. We use this feature in the analysis of the convergence of the iterative scheme.

[6] Our scheme is intended for multiphysics codes where Δt may be fixed by a "master" function at the start of the time step.

Proof Given $\beta \geq 0$ and requiring that the row sum of (22) be larger than a normalized nonnegative value yields,

$$d_j - N\,\gamma\,\Delta t\,\alpha_{k,j} \geq \Delta t\,\beta \geq 0\ . \tag{26}$$

Recalling (23) and (17), this leads to the inequality

$$a\,\tau^2 + b\,\tau + c \doteq p(\tau) \geq 0\ ,$$

where a, b, and c are defined in the lemma. If $\beta \leq 1$, then $a,\ b > 0$. Hence, if $c \geq 0$, then $p > 0$ for all τ. If $\beta > 1$, then sign(b) is indeterminate and for large Δt, c is negative. Nevertheless, given a large enough τ, we can assure that $p > 0$ since $a > 0$. The required value is that defined in (25). ▮

Diagonal dominance guarantees that A is an M-matrix, i.e., $A^{-1} > 0$. To ensure robustness, we derive conditions that guarantee nonnegativity of the RS of (22). The conditions form the basis of the following lemma.

Lemma 2 *Let*

$$\begin{aligned} a &= R\,\bar{\mu}_j\,v^i_{k,j}\ , \\ b &= R\,\bar{\mu}_j\,(\,v^i_{k,j} + v^0_{k,j}\,) + [\,p_{k,j}\,R\,T^i_k + \bar{\mu}_j\,v^i_{k,j}\,]\,\Delta t\ , \quad \text{and} \\ c &= R\,\bar{\mu}_j\,v^0_{k,j} + \{\,R\,[\,\alpha_{k,j}T^0_k + (p_{k,j} - \alpha_{k,j})T^i_k\,] + \bar{\mu}_j\,v^0_{k,j}\,\}\,\Delta t \\ &\quad + (p_{k,j} - \alpha_{k,j})\,T^i_k\,\Delta t^2\ . \end{aligned}$$

If $c \geq 0$, then the RS of (22) $w_{k,j} > 0$ for all $\tau \geq 0$. Otherwise, $w_{k,j} > 0$ if

$$\tau \geq (\,\sqrt{b^2 - 4ac} - b\,)/2a\ . \tag{27}$$

Proof We proceed as in Lemma 1. Substituting, (17) and (18) into (24) and normalizing yields a quadratic $q \doteq a\tau^2 + b\tau + c$, where a, b, and c are defined in the lemma. The inequality $q \geq 0$ is equivalent to $w_{k,j} \geq 0$. Since $a,\ b > 0$, if $c \geq 0$, then q is positive for all τ. Otherwise, τ must be greater than the (positive) root defined in (27). ▮

6 Level iteration scheme

Equation (22) is of the form $Av = w$ where v and w are vectors with components $v_{k,j}$ and $w_{k,j}$, respectively, and A is of the form

$$A = D - M_1 - M_2\ , \tag{28}$$

where $D = \mathrm{diag}(\,d_j + 2\eta_j - \gamma\,\Delta t\,\alpha_{k,j})$ and the (k,j) elements of the products

$$\begin{aligned} (M_1\,v)_{k,j} &= +\eta_j\,(v_{k-1,j} + v_{k+1,j}) \quad \text{and} \\ (M_2\,v)_{k,j} &= +\gamma\,\Delta t\,\alpha_{k,j}\sum_{\ell \neq j} v_{k,\ell}\ , \end{aligned}$$

where in the sum, the index ℓ ranges over all integers 1 to N except j. The splitting (28) suggests the following iterative scheme. Given an initial guess $v^{(i)}$, we obtain the next iterate in two steps,

$$(D - M_1)\, v^{(i+1/2)} = w + M_2\, v^{(i)} \tag{29}$$

$$(D - M_2)\, v^{(i+1)} = w + M_1\, v^{(i+1/2)} \ . \tag{30}$$

Equation (29) requires solving N separate, symmetric, positive definite linear systems, each of order K where K is the number of spatial grid points; while (30) reduces to K independent systems of order N, the number of groups for this level. Although the matrix on the LS of (30) is dense, since it is a rank one perturbation of a diagonal matrix, the inverse $(D - M_2)^{-1}$ is given explicitly using the Sherman–Morrison formula [10].

The exact solution v satisfies the above two equations with v replacing the superscripted variables. It follows that the error for the ith iterate,

$$e^{(i)} \doteq v - v^{(i)}$$

satisfies,

$$e^{(i+1)} = (D - M_2)^{-1}\, M_1\, (D - M_1)^{-1}\, M_2\, e^{(i)} \ . \tag{31}$$

Each matrix, $D - M_i$, is an M-matrix since it is obtained by setting certain off diagonal entries of A to zero, Varga [11], Theorem 3.12, p. 85. Hence, each splitting in (29) and (30) is a *regular splitting* of A, Varga [11], p. 88. Thus, each iteration (29) and (30) is individually convergent, Varga [11], Theorem 3.13, p. 89. That is, the spectral radii of the iteration matrices, e.g., of $(D - M_1)^{-1}\, M_2$, are less than one. This proves that the iteration (31) converges.

The convergence may be enhanced by a proper choice of the parameter β introduced in Lemma 1. To prove this, we examine (31) more closely. Consider the first half step,

$$(D - M_1)\, e^{(i+1/2)} = M_2\, e^{(i)} \ . \tag{32}$$

We express the error as a product of spatial and frequency components,

$$e^{(i)}_{k,j} \doteq \epsilon^{(i)}_j\, e^{\sqrt{-1}\, k\theta} \tag{33}$$

and similarly for $e^{(i+1/2)}$. Since $\epsilon^{(i)}$ is a linear combination of unit vectors, it suffices to analyze how one such vector is affected by the iteration. Let $\epsilon^{(i)} = \hat{\mathrm{e}}_m$, the N-dimensional unit vector. Since $||\epsilon^{(i)}|| = 1$, we seek a bound on $||\epsilon^{(i+1)}||$. Substituting into (32), yields

$$\epsilon^{(i+1/2)}_j = \frac{\gamma\, \Delta t \alpha_j}{d_j + 2\eta_j(1 - \cos\,\theta) - \gamma\, \Delta t\, \alpha_j} \ , \tag{34}$$

where we replaced $\alpha_{k,j}$ with α_j, a notation we adopt henceforth.

For the second half step,

$$(D - M_2)\, e^{(i+1)} = M_1\, e^{(i+1/2)} \ ,$$

let $e^{(i+1)}$ have form given in (33). Using the Sherman–Morrison formula, we obtain

$$\epsilon_j^{(i+1)} = \left(\zeta_j \, \epsilon_j^{(i+1/2)} + \frac{S_\zeta}{1 - S_a} \, a_j \right) \cos \theta \ , \tag{35}$$

where

$$\zeta_j = 2\eta_j/(d_j + 2\eta_j) \ , \qquad a_j = \gamma \, \Delta t \alpha_j/(d_j + 2\eta_j) \ , \tag{36}$$
$$S_\zeta = \sum_{\ell=1}^{N} \zeta_\ell \, \epsilon_\ell^{(i+1/2)} \ , \quad \text{and} \quad S_a = \sum_{\ell=1}^{N} a_\ell \ .$$

The diagonal dominance criterion (26) ensures that $\epsilon_j^{(i+1/2)} \geq 0$. The terms ζ_j and a_j are clearly nonnegative. We will show that $S_a < 1$; hence, the parenthetical expression in (35) is nonnegative. Summing the components yields

$$||\epsilon^{(i+1)}||_1 = \sum_{j=1}^{N} |\epsilon_j^{(i+1)}| = |\ \cos \theta \,|\, S_\zeta \,/\, (1 - S_a) \ .$$

And so we seek an upper bound for $|\cos \theta \,|\, S_\zeta$ and a lower bound for $1 - S_a$.

For $(1 - S_a)$, diagonal dominance (26) and the definition of a_j imply that

$$a_j \leq \gamma \, \alpha_j/(\beta + \gamma \, N \, \alpha_j + \xi_j) \ , \tag{37}$$

where

$$\xi_j \doteq 2\eta_j/\Delta t = 2\hat{\mu}_j \, \bar{\mu}_j/h^2 \ .$$

Since $\hat{\mu}_j$ and $\bar{\mu}_j$ are bounded by the cube of the frequency mesh$\{\, \nu_j\}$, the variable $\xi_j \approx 2\nu_j^6/h^2$. Hence, ξ_j may be arbitrarily small or large. The inequality (37), the definition of S_a, and (20) yield

$$\begin{aligned} 1 - S_a &\geq \sum_j \alpha_j - \sum_j \gamma \, \alpha_j/(\beta + \gamma \, N \, \alpha_j + \xi_j) \\ &= \sum_j \alpha_j \, (\, \beta - \gamma + \gamma \, N \, \alpha_j + \xi_j \,)/(\beta + \gamma \, N \, \alpha_j + \xi_j \,) \ . \end{aligned}$$

To bound $|\cos \theta \,|\, S_\zeta$, we apply diagonal dominance (26) on the terms $\epsilon_j^{(i+1/2)}$ and ζ_j, defined in (34) and (36) respectively, and obtain

$$|\cos \theta \,|\, S_\zeta \leq \sum_j \left(\frac{\xi_j}{\beta + \gamma \, N \, \alpha_j + \xi_j} \right) \left(\frac{\gamma \, \alpha_j}{\beta + \gamma \, (N - 1) \, \alpha_j} \right) \ .$$

In deriving the inequality, we assumed the most pessimistic possibility $\theta = 0$.

We now derive a simple result. Let x_j, y_j, z_j denote the respective, positive components of three vectors and let ω be a positive scalar. If for each component

$$y_j < \omega \, z_j \ , \tag{38}$$

then

$$\left(\sum_j x_j\, y_j\right) \Big/ \left(\sum_j x_j\, z_j\right) < \omega\ . \tag{39}$$

By letting

$$\begin{aligned} x_j &= \alpha_j \,/\, (\beta + \gamma\, N\, \alpha_j + \xi_j)\,, \\ y_j &= \gamma\, \xi_j \,/\, (\beta + \gamma\, (N-1)\, \alpha_j)\,, \quad \text{and} \\ z_j &= \beta - \gamma + \gamma\, N\, \alpha_j + \xi_j\,, \end{aligned}$$

we note that that the bounds on $|\cos\theta|\, S_\zeta/(1-S_a)$ are precisely as on the LS of (39). If we assume that $\omega < 1$, (38) is equivalent to

$$0 < \omega\,(\,\beta - \gamma + \gamma\, N\, \alpha_j\,)\,[\,\beta + \gamma\,(N-1)\,\alpha_j\,] + \xi_j\,\{\,\omega\,[\,\beta + \gamma\,(N-1)\,\alpha_j\,] - \gamma\,\}$$

Since $\alpha_j = O(1/N)$, this reduces to

$$0 < \omega\,(\,\beta + \gamma\,\varepsilon\,)\,[\,\beta + \gamma\, O(1)\,] + \xi_j\,\{\,\omega\,[\,\beta + \gamma\, O(1)\,] - \gamma\,\}\ ,$$

where ε denotes a number small in relation to one. The RS consists of two terms; the one independent of ξ_j is clearly positive (or can be made to be for β near one. The other term is positive if we choose β satisfying

$$\beta > \max\{\,0, \gamma\,[\,1/\omega - O(1)\,]\,\}\ . \tag{40}$$

We have proved:

Lemma 3 *Given $\omega \in (\,0,\,1)$, if β satisfies (40), the two–step iteration scheme (29)–(30) converges and the spectral radius of the iteration matrix is bounded by ω.*

Equation (40) is the desired relation. For small Δt, $\gamma \approx 0$ and simple diagonal dominance, i.e., $\beta \approx 0$, suffices. For large Δt, $\gamma \to 1$ and we need much stronger diagonal dominance to ensure that (31) converges. In particular, if $\gamma = 1/2$ and we wish to guarantee that the error is halved each time, we should use $\beta = 1$. Of course, a large β necessitates a large τ implying a smaller Ψtc time step, i.e., it will take longer to reach the desired steady state (14)–(15).

7 Results

We now apply the scheme to two test problems. In the first, we simulate the decay of a localized hot spot. In the second, we compute the propagation of a "Planckian" radiation flux (defined below) into cold matter. The problems exemplify common applications of the radiation diffusion equations, e.g., as the vehicle by which energy streams through matter.

We will compare solutions of the one group equations, (8) and (9), with those of the multigroup system, (6) and (7). For the latter, we present solutions using $\mathcal{N} = 2, 4, \ldots,$ 64 groups. The multigroup results consist of distinct simulations; each an application of the scheme described above. Thus, the 4 group simulation begins each time step by advancing the one group equations. The result forms the initial iterate for a two group level; the guess is improved using the inner/outer iterative scheme. The converged two group level result is then interpolated to obtain the initial guess for the (finest) four group level. The 8 group simulation is similar, except in this case, the finest level uses eight groups. Hence, after converging the four group level, the result forms the initial iterate for the eight group level. Although results using a small number of groups are of limited physical interest, they are presented in order to demonstrate convergence as $\mathcal{N}$ is increased.

Each multigroup simulation discretizes the same range of the frequency coordinate. We first define a "base" geometrically spaced grid of 64 intervals, $\nu_{j+1} - \nu_j = 1.15\,(\nu_j - \nu_{j-1})$, with $\nu_1 = 5 \cdot 10^{-4}$; hence, $\nu_{64} = 25.5555$ The base grid is the finest level grid for the 64 group simulation. The next coarse level grid is obtained by combining two adjacent fine level intervals yielding a discretization of 32 intervals and spanning the same frequency range. This mesh also forms the finest level grid for the 32 group simulation. Hence, the first nonzero frequency for the 32 group simulation is $(1 + 1.15) \times 5 \cdot 10^{-4}$. The process is repeated down to the level (and simulation) using two groups. Thus, the two group mesh is given by $\{\nu_j\} = \{\,0, 0.2886, 25.5555\}$.

The spatial domain is discretized using a fixed width, $h = 1/50$. Simulations using finer spatial meshes yield approximately the same results. We chose $h = 1/50$ in order to display values as separate symbols; a finer mesh blurs the plots.

7.1 Decay of localized matter energy

We consider the same problem parameters as those used by Shestakov [12]. The initial temperature has the peaked profile:

$$T|_{t=0} = \begin{cases} 6.4775\,, & \text{if } |x| < 0.04 \\ 0.0027\,, & \text{otherwise} \end{cases} .$$

The initial radiation energy density is constant, $E|_{t=0} = 5.2344 \cdot 10^{-7}$. The matter "specific heat" $R = 2.0$. We define the matter $\mathcal{E}_m(t)$ and radiation $\mathcal{E}_r(t)$ energies,

$$\mathcal{E}_m = R \int dx\, T \quad \text{and} \quad \mathcal{E}_r = \int dx\, E = \int dx \int d\nu\, u\ .$$

The initial conditions stipulate that $\mathcal{E}_m|_{t=0} = 1.0469$ and $\mathcal{E}_r|_{t=0} = 1.0469 \cdot 10^{-6}$. The computational domain is $|x| < 1$. At the boundaries, homogeneous Neumann conditions are imposed. Hence, the total energy $\mathcal{E} = \mathcal{E}_m + \mathcal{E}_r$ is constant in time. However, the individual quantities, $\mathcal{E}_m$ and $\mathcal{E}_r$, vary with t as the fields exchange energy. The steady state fields are independent of x, and $\mathcal{E}_m = 1$.

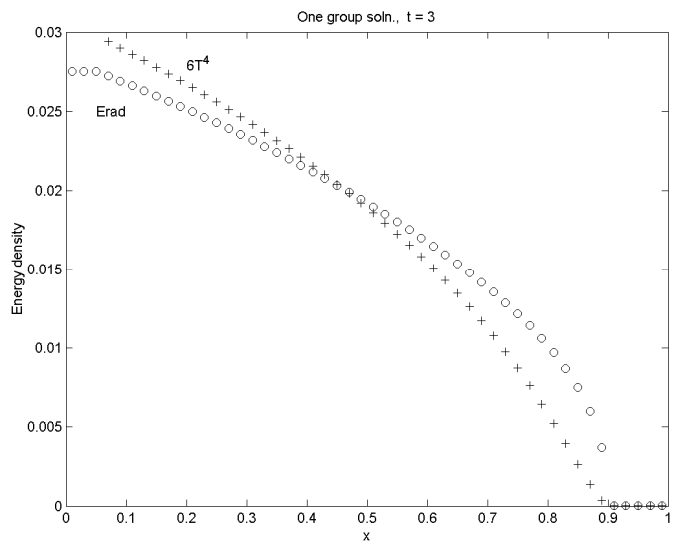

Figure 2: Central T problem. One group solution. Radiation energy E and emission source $6T^4$ vs. x, $t = 3.0$

We first consider the one group equations, i.e., (8) and (9). Figure 2 displays the energy E and emission source $6T^4$ at $t = 3$. Due to symmetry, we present results only for $x > 0$. Except near $x = 0$, the two fields are tightly coupled over the spatial domain. The figure shows that the initial temperature spike has transformed into an outgoing wave which at $t = 3$ has reached $x = 0.9$ The solution confirms the analysis given at the end of section 1, viz., wherever T is small, the fields are tighly coupled.

Since T retains remnants of its initial, peaked profile at the origin, we exclude the central values of $6T^4$ from the figure. For reference, at $t = 3$, the first few values of $6T^4$ are 26.4600, 26.4600, and 0.0298; hence, the central temperature has decayed nearly fivefold, from $T = 6.4775$ to $T = 1.4491$

The temporal histories of $\mathcal{E}_m$ are displayed in Fig. 3. For the one group solution, the result confirms our expectation, $\mathcal{E}_m$ is always larger than $\mathcal{E}_r$. In fact, $\mathcal{E}_m$ monotonically approaches the equilibrium value.

Figure 3 also displays $\mathcal{E}_m(t)$ for various multigroup solutions. These are separate simulations of (6) and (7) using $\mathcal{N} = 4, 8$, etc. groups. There are two noteworthy items. First, is the striking difference between the multigroup solutions and those using only one group. All multigroup $\mathcal{E}_m$ undergo a sharp initial decrease, falling to less than half of the equilibrium value, before recovering and beginning a slow, steady rise. Secondly, the figure shows an obvious convergence as the frequency grid is refined. We note that the 64 group $\mathcal{E}_m$ agrees with that presented in [12], Fig. 8. The multifrequency equations provide a means for matter energy, initially at $x = 0$, to radiate into the high frequencies and quickly diffuse away. High frequencies are characterized by slow

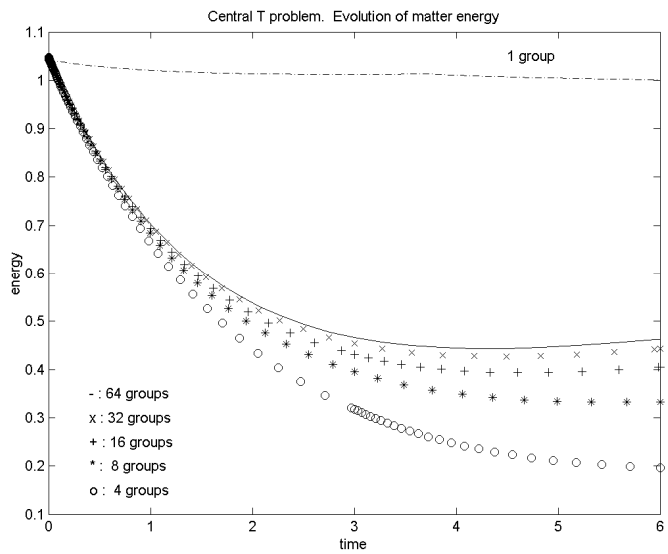

Figure 3: Central T problem, Temporal histories $\mathcal{E}_m(t)$ for 1 group and various multi-group simulations.

absorption.

We conclude this section with Fig. 4 which displays the radiation energy density E at $t = 3$ for various multigroup simulations. We again see convergence as the number of groups $\mathcal{N}$ is increased. In comparing these results with the one in Fig. 2, we note the larger value of the multifrequency E and, for $\mathcal{N} \geq 16$, its near uniformity with x.

7.2 Radiation into cold matter

Here we simulate the transport of radiation into cold matter. The specific heat $R = 10$ Initially, $T = 0.001$ and $E = E^0 = 10^{-6}$. For the multigroup simulations, we initialize the group energies by first defining the initial "radiation temperature" $T_r^0 = (E^0/6)^{1/4}$, then compute group energies according to the profile $\nu^3 \exp(-\nu/T_r^0)$. The spatial domain is $0 < x < 1$. On the boundaries we impose the condition,

$$a\,E - F \cdot \hat{n} = c\ ,$$

where $F = -210T^3\nabla E$ is the radiation flux, a and c are constants, and $\hat{n}$ is the outward normal. Hence, $-F \cdot \hat{n}$ denotes the incoming flux. For the multigroup equations, the flux is assumed to have a "Planckian," i.e., $\nu^3 \exp(-\nu/T)$ profile, which stipulates the fluxes that each group receives. At $x = 0$, we set $a = c = 1$, while at $x = 1$, we set $a = 1$ and $c = 0$. In early times, the $x = 0$ boundary condition effectively imposes an incoming unit flux of energy into the problem; in late times, it sets the Dirichlet condition $E = 1$. The $x = 1$ condition allows energy to stream out of the problem.

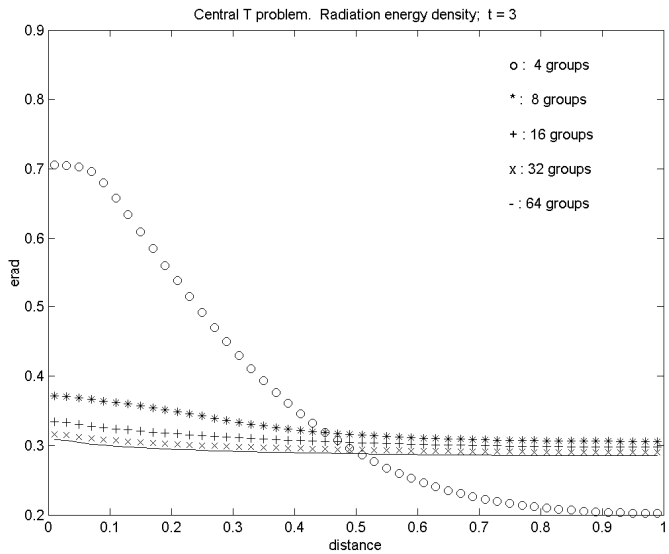

Figure 4: Central T problem, Radiation energy density E vs. x at $t = 3$.

Figures 5 and 6 display the radiation energy density E and matter temperature T at $t = 1$, respectively. In Fig. 6, we plot $T/20$ for the one-group simulation in order to fit the result within the multigroup bounds. As in the previous problem, we see a striking contrast between the one-group and multigroup simulations and note a distinct convergence as $\mathcal{N}$ is increased. The one-group calculation is characterized by a steep wave front, which at $t = 1$ has propagated to $x \approx 0.38$ Also, E and B are concave down, giving the appearance of energy "bottling up" rather than streaming through the material. In contrast, the multigroup E is concave up; the high frequency energy readily passes through the domain.

8 Summary and conclusion

We have presented a scheme to solve the multigroup radiation diffusion equations. Although the scheme has been analyzed and applied to the H&S model [1], it is intended for the more general set of equations governing multifrequency radiation diffusion. The scheme consists of several straightforward steps, which when combined, make a powerful tool. The basic premise is that if a problem requires a large number of groups, the formidable set of $\mathcal{N}$ coupled diffusion equations is advanced by bootstrapping from a smaller number of groups spanning the same frequency range. That is, we apply multigrid to the frequency range.

The scheme may be easily modified and it is useful to suggest extensions and pos-

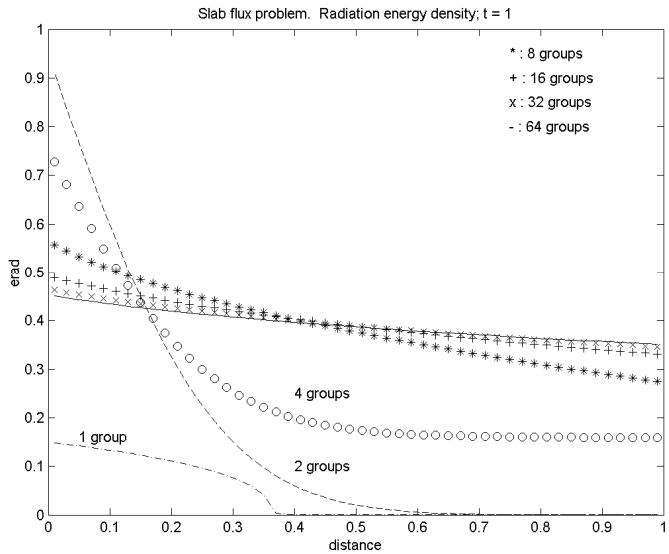

Figure 5: Incoming flux problem, Radiation energy density E vs. x at $t = 1$.

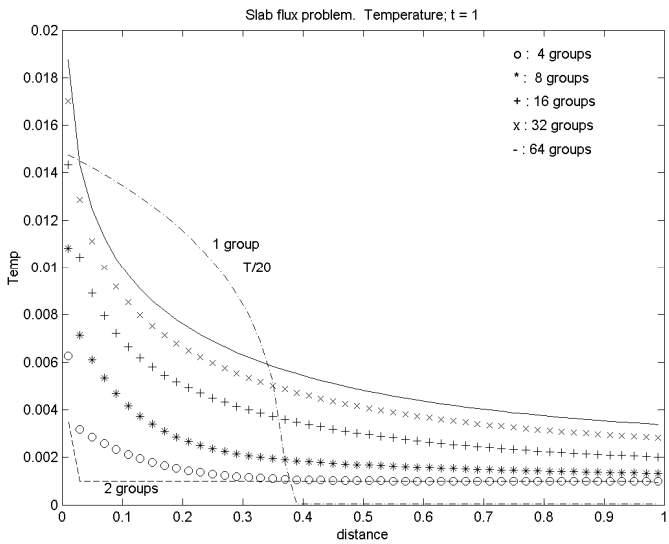

Figure 6: Incoming flux problem, Matter temperature T vs. x at $t = 1$.

sible improvements. For example, our multigrid approach is based on the concept that the solution for a coarse level of groups is a good estimate for the fine level. However, for the coarsest level, the results of section 7 do not support the hypotheses since solutions of the one group and two group equations are so different. Thus, it may be wiser to dispense with the one group level and initiate each time step with a coarsest level consisting of two, possibly even four, groups.

As presented, the scheme is nonlinear. Each level consists of an inner/outer iterative scheme. The inner iterations solve a linearization of the equations while for the outer ones, material properties such as opacities are recomputed. For some applications, the evaluation of material properties may be prohibitively expensive. If so, the scheme may still be applied by not recomputing the coefficients. However, for a simulation using $\mathcal{N}$ groups, the scheme does require coarse group averaged opacities.

Although our presentation coarsened each frequency range by a factor of two, this is not a requirement. For example, if a problem consisted of a material for which it is essential to properly discretize a particular frequency range, one may coarsen the less interesting ranges more aggressively.

Within each level, we solve a nonlinear set of equations using an inner/outer iterative scheme. By introducing pseudo transient continuation Ψtc, the inner iterations are viewed as successive approximations to a steady state. The inverse of the Ψtc time step τ brings an extra degree of robustness. The iterations are stable. Each iterate is physically reasonable; there is no concern about subsequent evaluations of material properties with say, a negative temperature.

The inner/outer iterations do not need to be solved to great accuracy. Indeed, for the coarsest levels, doing so simply yields a correct answer to the wrong problem. However, we stress that whatever tolerance is chosen for the inner/outer iterations, the levels conclude with an additional step guaranteeing energy conservation. This we do as follows. After the inner/outer iterations are deemed to be sufficiently converged, we recompute the $\hat{\mu}_j$, $\bar{\mu}_j$, and p_j coefficients using the latest temperature $T^{(i)}$. These values, when inserted into (14) yield N independent equations for u_j, where we also set $T = T^{(i)}$. After obtaining the energy densities at the advanced time, the new temperature (for the current level) is then,

$$T = T^0 + \frac{\Delta t}{R} \left(-T^{(i)} + \sum_{j=1}^{N} u_j/\bar{\mu}_j \right) . \tag{41}$$

The procedure is clearly energy conserving. The energies u_j are nonnegative since they are solutions of linear systems $Ax = b$ where each A is an M matrix and each b consists of nonnegative components. The only concern is that T may be unphysical (too low, or even negative) if $(\Delta t\, T^{(i)}/R)$ is large in relation to the other terms. The computer program monitors for such events and signals if this occurs. If it does, T is reset to a minimum value, which ruins energy conservation. So far we have yet to witness such an event. Our results conserve energy, nearly to round off. However, note that even if (41) were to yield a negative T for an intermediate level, hope is not lost since the result is only needed as an initial guess for the next finer level.

Although we chose to apply multigrid only to the frequency range, one may experiment by also applying it to the spatial domain. Our scheme may be generalized to multiphysics programs using automatic (spatial) grid refinement (AMR). In such cases, the coarse frequency levels may be advanced on coarsened spatial grids.

Finally, recalling the scheme of Axelrod et al [5], we list a few extensions. The H&S model to which we applied our scheme was derived by ignoring processes such as Compton scattering and radiation pdV work. The former reduces to a diffusion equation in frequency space. Radiation pdV is included when coupling radiation transport to hydrodynamic motion. In regions where the fluid is compressed (rarefied), radiation energy is transferred to higher (lower) frequencies. The process is modeled as a translation in frequency space, $\partial_t u = a\,\nu\partial_\nu u$, where sign($a$) depends on sign($dV$). Both processes may be incorporated into our scheme. For stability, we would insist on approximating the pdV process with upwinding. Thus, the dual matrix splitting inner iterations can still be used. The only complication is that the M_2 matrix would no longer be a rank one perturbation of a diagonal matrix. Hence, the Sherman Morrison formula cannot be used. The second splitting requires inverting a full matrix of size N at each spatial grid point.

A Analysis of $\bar{\nu}_j$ and $\hat{\nu}_j$

Lemma 4 *The coefficients $\bar{\nu}_j$ and $\hat{\nu}_j$ satisfy (4).*

Proof Since the proof for $\hat{\nu}_j$ is similar to the one for $\bar{\nu}_j$, we only present the latter. Let $y_j = \nu_j/T$. If $y \in (\, y_{j-1},\, y_j)$, it follows that

$$y_{j-1}^3 \int_{y_{j-1}}^{y_j} dy\, e^{-y} < \int_{y_{j-1}}^{y_j} dy\, y^3\, e^{-y} < y_j^3 \int_{y_{j-1}}^{y_j} dy\, e^{-y}\ .$$

If we divide the inequalities by $\int_{y_{j-1}}^{y_j} dy\, e^{-y}$, multiply by T^3, and recall the definition (10), we obtain,

$$\nu_{j-1}^3 < \bar{\mu}_j < \nu_j^3\ ,$$

which is equivalent to what we need. ∎

B Solution of "one group" system

Here we describe the scheme for the coarsest level, i.e., the one used to solve (8)–(9). By defining

$$B \doteq 6T^4\ ,$$

we rewrite (9) as:

$$(R/4)\,\partial_t B = -(\,B - E\,) \tag{42}$$

Since (8)–(9) is nonlinear, iteration is required. Let B^0 and E^0 respectively denote the emission source and radiation energy at the previous time level and let $B^{(i)}$ and $E^{(i)}$ respectively denote the i-th iterates approximating the new source and radiation energy. The iteration begins by assigning $B^{(0)} = B^0$.

Assuming $E^{(i)}$ is known, backward Euler differencing of (42) yields,

$$B^{(i)} = \varpi\, B^0 + (1 - \varpi)\, E^{(i)} \tag{43}$$

where

$$0 < \varpi = R/(R + 4\Delta t) < 1 \ .$$

Equation (43) is robust; the new source is an average of the new radiation energy and the source at the previous time level. If both B_0 and $E^{(i)}$ are nonnegative, so is $B^{(i)}$. We define

$$T^{(i)} \doteq (B^{(i)}/6)^{1/4} \tag{44}$$

and substitute the latest known T into (8). Backward Euler differencing leads to the equation for $E^{(i)}$, viz.,

$$\begin{aligned} &-\Delta t\, \partial_x [\, 210 (T^{(i-1)})^3\, \partial_x E^{(i)}\,] \\ &\qquad + \left(1 + \frac{\varpi \Delta t}{6 (T^{(i-1)})^3} \right) E^{(i)} = E^0 + \frac{\varpi \Delta t\, B^0}{6 (T^{(i-1)})^3} \ . \end{aligned} \tag{45}$$

This equation is also robust. The diffusion coefficient, lower order term, and right hand side (RS) are nonnegative. With proper differencing we obtain a linear system with an M matrix. Thus, the new energy $E^{(i)}$ is guaranteed to be nonnegative.

The iterations are done in the following order. We set $i = 1$ and solve (45) to obtain $E^{(1)}$. Then, (43)–(44) yield the new emission and temperature. We increment i and continue solving (45), (43), and (44), in that order. We iterate until the iteration error

$$\varepsilon \doteq \frac{||T^{(i)} - T^{(i-1)}||}{||T^{(i)}||}$$

is reduced to a specified tolerance.

The tolerance ε need not be overly restrictive since the goal is not to solve (8)–(9) exactly, but rather to only obtain a good initial guess for the next fine level system, i.e., the one using two groups. Typically, it suffices to iterate only up to $i = 2$. However, before leaving the coarsest level, we perform an additional step.

The iterate pair $(\, E^{(i)},\, T^{(i)})$ does *not* conserve energy. It is easy to check that

$$\Delta t\, (\, E^{(i)} - B^{(i)}\,)/[6 (T^{(i-1)})^3]$$

is the energy density that is taken out of the E field during the time step and that this amount does not equal the matter energy change,

$$R\, (\, T^{(i)} - T^0\,) \ .$$

Hence, to conserve energy, we compute

$$T^{(*)} = T^0 + (\Delta t/R)\,(\,E^{(i)} - B^{(i)}\,)\,/\,[6(T^{(i-1)})^3]\ .$$

Unfortunately, there is no guarantee that $T^{(*)}$ is physically reasonable, e.g., positive.[7] Thus, if we have specified a minimum temperature $T_{\min}$ (zero default), in cells where $T^{(*)}$ is too low, we reset it, thereby obtaining the final coarse level temperature

$$T^{(f)} = \max(\,T_{\min},\, T^{(*)}\,)\ .$$

As a final check, we monitor the energy "lost,"

$$E_{m,\mathrm{lost}} = R\int dx\ \max(\,0,\, T_{\min} - T^{(*)})\ .$$

We have yet to find a problem which generates a nonzero $E_{m,\mathrm{lost}}$.[8] Note that it is not imperative to exit coarse levels with energy conserving fields since coarse level solutions are only used as initial guesses for subsequent fine levels.

This concludes the description of the scheme for the coarsest level. The result consists of the fields $T^{(f)}$ and $E^{(i)}$. The latter is interpolated to a 2–group field per the algorithm described in section 2.

Acknowledgment. We extend our gratitude to Prof. A. Greenbaum of the Univ. of Wash. for suggesting the Sherman Morrison formula. We also thank Prof. O. Hald of the Univ. of Calif., Berk., Prof. J. Wilkening of New York Univ., Dr. P. Concus of the Lawrence Berk. Lab., and Dr. J. Bolstad of the Lawrence Livermore Natl. Lab. for numerous useful discussions. Numerical results were generated using Matlab.

References

[1] O. H. Hald and A. I. Shestakov, "Stability of stationary solutions of the multifrequency radiation diffusion equation," Lawrence Livermore Natl. Lab. UCRL-JC-148079, (2002), submitted to *SIAM J. Appl. Math.*

[2] Ya. B. Zel'dovich and Yu. P. Raizer, *Physics of Shock Waves and High-Temperature Hydrodynamic Phenomena*, Academic Press, New York, 1966

[3] E. M. Lund and J. R. Wilson, unpublished, Report UCRL-84678, Lawrence Livermore Natl. Lab., Livermore, CA (July 1980)

[4] A. I. Shestakov, J. A. Harte, and D. S. Kershaw, "Solution of the diffusion equation by finite elements in Lagrangian hydrodynamic codes," *J. Comp. Phys.*, **76**, 2, (1988)

[7] Or, bounded from above.

[8] Or, one in which $T^{(*)}$ is unphysically large.

[5] T. S. Axelrod, P. F. Dubois, and C. E. Rhoades Jr. "An implicit scheme for calculating time– and frequency–dependent flux limited radiation diffusion in one dimension," *J. Comp. Phys.*, **54**, 2, 205–220, (1984)

[6] A. Friedman and D. S. Kershaw, "Fully implicit solution of coupled multigroup radiation diffusion and electron temperature equations," in *1982 Laser Program Annual Report*, UCRL-50021-82, Lawrence Livermore Natl. Lab., Livermore, CA, p. 3-68 (Aug. 1983)

[7] J. E. Morel, E. W. Larsen, and M. K. Matzen, "A synthetic acceleration scheme for radiative diffusion calculations," *J. Quant. Spectrosc. Radiat. Transfer*, **34**, 3, 243–261 (1985)

[8] A. I. Shestakov, J. A. Greenough, and L. H. Howell, "Solving the radiation diffusion and energy balance equations using Pseudo Transient Continuation," Lawrence Livermore Natl. Lab. UCRL-JC-138727, Rev. 1, (2002), submitted to *J. Comp. Phys.*

[9] J. I. Castor, private communication, Lawrence Livermore Natl. Lab. (2002)

[10] G. H. Golub and C. F. Van Loan, *Matrix computations*, John Hopkins Univ. Press, Baltimore, Maryland, 1983

[11] R. S. Varga, *Matrix Iterative Analysis*, Prentice-Hall, Inc., Englewood Cliffs, New Jersey, 1962

[12] A. I. Shestakov, "Solving the multifrequency radiation diffusion equations using Branching Brownian motion," Lawrence Livermore Natl. Lab. UCRL-JC-149411, (2002), submitted to *J. Comp. Phys.*